Journal of Sound and Vibration (1997) **200**(2), 139–149

ERROR MEASURES FOR THE FINITE STRIP VIBRATION ANALYSIS METHOD

D. B. Stephen and G. P. Steven

Finite Element Analysis Research Centre, Building J07, Engineering Faculty, University of Sydney, N.S.W. 2006, Australia

(*Received* 2 *January* 1996, *and in final form* 2 *May* 1996)

The finite strip method is a useful tool for the determination of the buckling load factor and natural frequency for a given cross-section of a member. This method has the advantage of producing accurate results for a relatively coarse mesh when compared with the finite element method. This paper demonstrates a procedure to improve the natural frequency estimation and use it to give an accurate prediction for the error of the finite strip solution.

1. INTRODUCTION

Natural frequency and buckling analysis of thin plate structures is generally considered to be either plate local effects or flexural, torsional, or flexural-torsional deformation of the member. Plate local vibration analysis assumes that the line junctions between intersecting plates remains straight, and the member vibration assumes that the cross-section remains undistorted. The finite strip method [1] overcomes both of these assumptions and produces quite accurate results as both local and member natural frequency and buckling can occur simultaneously using the finite strip method. A combination of local and member effects for buckling has been termed as distortional [2] and can be similarly used for the natural frequency analysis of a structure. This paper examines the errors associated with natural frequency analysis. The errors associated with the finite strip buckling have been examined previously [3].

The finite strip method involves discretizing the structural membrane being examined into a series of flat strips to represent the structure. See Figure 1. From these strips the global elastic stiffness and mass matrices are created.

The natural frequency is given by the square root of the eigenvalue λ in the eigen equation (1):

$$([K] - \lambda[M])\{x\} = \{0\}, \tag{1}$$

where $[K]$ and $[M]$ are the global elastic stiffness and mass matrices respectively, and $\{x\}$ is the eigenvector that represents the displaced shape of the structure. The eigenvalue can also be determined using the Rayleigh quotient shown in equation (2):

$$\lambda = \frac{\{x\}^{\mathrm{T}}[K]\{x\}}{\{x\}^{\mathrm{T}}[M]\{x\}} \tag{2}$$

which is used later in this paper for the derivation of the improve eigenvalue.

0022–460X/97/070139 + 11 $25.00/0/sv960614

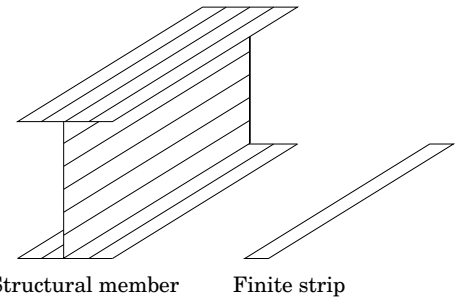

Figure 1. Discretization of a structural member into finite strips.

There is little work in the area of error estimation for the finite strip method. Error estimation techniques for the finite element method such as those by Friberg *et al*. [4, 5] and Cook [6, 7] have not generally been used for the finite strip method as they have only limited success with the finite element method.

2. DERIVATION OF FINITE STRIP MATRICES

In order to improve the eigenvalue obtained from a finite strip analysis it is necessary to briefly review the basic principles of the formulation of the local elastic stiffness and mass matrices. The finite strip is separated into two types of deformation behaviour: flexural and membrane deflections.

2.1. FLEXURAL DEFLECTION

The flexural displacement has two degrees of freedom associated with each node, namely the vertical, out-of-plane displacement and the rotation of the node. Along the length of the strip the method assumes a sine curve for the displacement which corresponds to the half wave length of the buckles (see Figure 2).

Across the strip the flexural displacement is a polynomial of order three as shown in equation (3). This has four unknowns relating to the four degrees of freedom.

$$N_f = \alpha_{v1} + \alpha_{v2}x + \alpha_{v3}x^2 + \alpha_{v4}x^3. \tag{3}$$

Combined with the sine curve displacement the shape function for the flexural component of the finite strip is:

$$N_F = N_f \sin(\pi z/L). \tag{4}$$

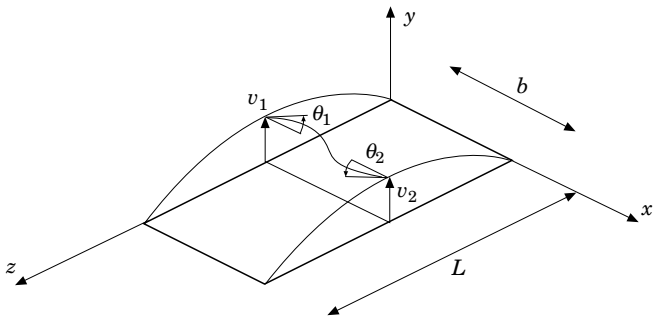

Figure 2. Flexural displacement for the finite strip.

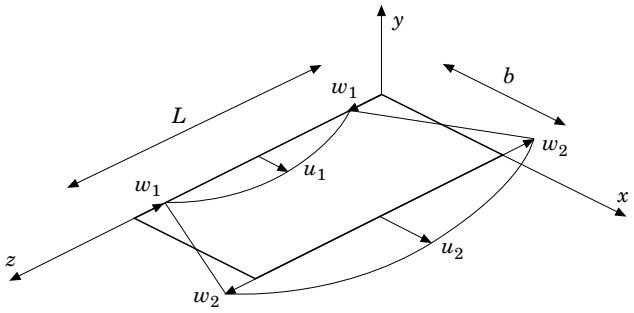

Figure 3. Membrane displacement for the finite strip.

The formulation of the flexural elastic stiffness matrix follows standard finite element routines.

$$[K_F] = \int_A [B_F]^T [D_F][B_F]\, dA, \tag{5}$$

where $[B_F]$ is the strain matrix derived by the second differential of the shape function corresponding to curvatures of the plate, and $[D_F]$ is the materials properties matrix for plate bending. The integration is over the surface area of the strip with $dA = dx\, dz$.

The flexural consistent mass matrix is:

$$[M_F] = \int_A [N_F]^T \rho [N_F]\, dA, \tag{6}$$

where $[N_F]$ is the flexural shape function, and ρ is the density of the material.

2.2. MEMBRANE DEFLECTION

The membrane displacement has two degrees of freedom associated with each node, being the orthogonal displacements parallel to the strip in the line of the strip and across the strip. Also, along the length of the strip the method assumes a sine curve for the displacement in the x direction. In the z direction the deformation is at the ends of the strip as opposed to the centre, hence a cosine curve is used for this deformation along the length of the strip (refer to Figure 3).

Across the strip the membrane displacements u and w are independent; as a result there is a separate polynomial function of order one to represent their individual displacements.

$$N_{m,u} = \alpha_{u1} + \alpha_{u2} x, \qquad N_{m,w} = \alpha_{w1} + \alpha_{w2} x. \tag{7, 8}$$

The addition of the trigonometric functions for the displacement along the length of the member results in two shape functions:

$$N_{M,u} = N_{m,u} \sin(\pi z/L), \qquad N_{M,w} = N_{m,w}(L/\pi) \cos(\pi z/L). \tag{9, 10}$$

The formulation of the membrane elastic stiffness matrix again follows the standard finite element routines.

$$[K_M] = \int_A [B_M]^T [D_M][B_M]\, dA, \tag{11}$$

where $[B_M]$ is the membrane strain matrix derived from the first differential of both of the membrane shape functions and $[D_M]$ is the materials properties matrix for plane-stress membrane behaviour. The membrane consistent mass matrix is:

$$[M_M] = \int_A [N_M]^T \rho [N_M] \, dA, \tag{12}$$

where $[N_M]$ is a combination of the x- and z-axis deformation shape functions.

The flexural and membrane elastic stiffness and mass matrices undergo the necessary transformations and are assembled into the global elastic stiffness and mass matrices of equation (1).

3. EIGENVALUE IMPROVEMENT

The results of a finite strip analysis, like the finite element method, can be improved by refining the mesh used in the analysis model. This requires extra work and can become time consuming for the resolving of the problem. Based on previous work by the authors [3, 8, 9] the eigenvalue for the finite strip method can be improved *without* resolving the refined model. Each element in the original model is examined and individually subdivided. The new eigenvector for this refined mesh is derived from the original eigenvector on the element and surrounding elements. These surrounding elements with the central elements are called the *patch* of elements.

A polynomial higher than the original finite element shape functions is derived using the eigenvector displacements for the nodes in the patch. A higher order polynomial is used to produce a more accurate deformed shape over the finite strip patch of element. There are principally three shape functions for the finite strip element, one for the flexural displacement and two for the membrane displacement, as shown by equations (4), (9) and (10).

Only elements in the same line may be considered in the patch as the polynomial is calculated in a linear axis form. The structure behaves quite differently across bends in the cross-section due to the generally large difference in values between the flexural and membrane stiffness of the plate. For a patch using these elements there is either a three element patch for the typical patch in a straight section of elements or two elements in a patch for elements at a boundary or a corner in the structure as shown in Figure 4.

The vertical displacement shape function N_F related to the flexural displacement of the finite strip has a polynomial of order three. The two membrane displacements $N_{M,u}$ and $N_{M,w}$ have a polynomial of order one. For the finite strip method a patch of elements may consist of either two or three elements. Figure 5 shows the number of degrees of freedom associated with the patch possibilities and shape functions. The order of the polynomial used for the patch displacement function is based upon the number of degrees of freedom in the patch. As there are more nodes in the patch than the original element, the order

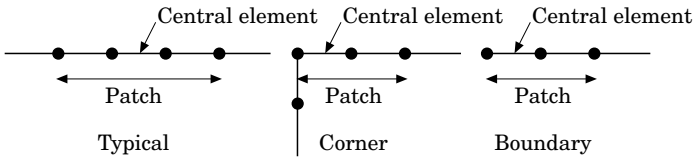

Figure 4. Definition of patches for various locations.

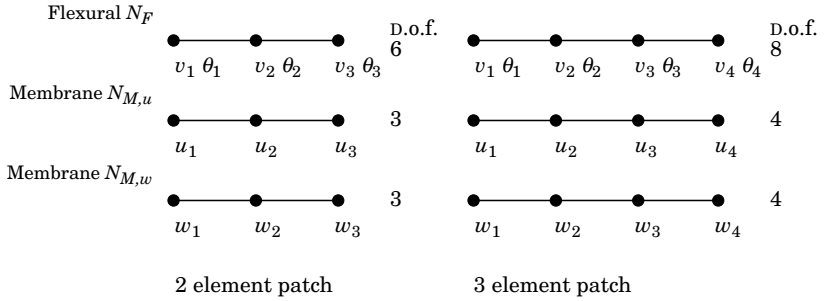

Figure 5. Patch displacements for the finite strip.

of the polynomial will be larger than the original finite strip element shape function. See Figure 6.

A new eigenvector $\{x^*\}$ can be derived for the sub-elements of the central element of the patch using the patch displacement function. The new eigenvector can be used in the Rayleigh quotient of equation (2) to calculate the new eigenvalue λ^*. The Rayleigh quotient can be calculated by summing the number and denominator terms for individual elements, and hence this process can be performed at an individual element level.

Although the new eigenvector is derived from a higher order function than the original finite strip solution, the associated improved eigenvalue is not guaranteed to be exact and is best used as an error measure for the original results. The finite element analysis error can be calculated knowing the exact eigenvalue λ_{EX} as:

$$\varepsilon = (\lambda - \lambda_{EX})/\lambda_{EX}. \tag{13}$$

Using the improved eigenvalue the error measure can be calculated as:

$$\varepsilon^* = (\lambda - \lambda^*)/\lambda^*. \tag{14}$$

If the improved eigenvalue is more accurate than the original eigenvalue obtained from the finite strip analysis then the error measure will be quite accurate.

4. EXTRAPOLATION OF EXACT SOLUTION

The calculation of the exact natural frequency cannot be achieved with a finite number of strips in the analysis due to the incapacity of the polynomial shape functions to represent perfectly the complex deformed shape. However, as the mesh is refined the finite strip solution will approach the exact solution as a limit. This is supported by the fact that the errors for the finite strip analysis using different mesh refinements will converge uniformly on a log-log plot as shown in Figure 7.

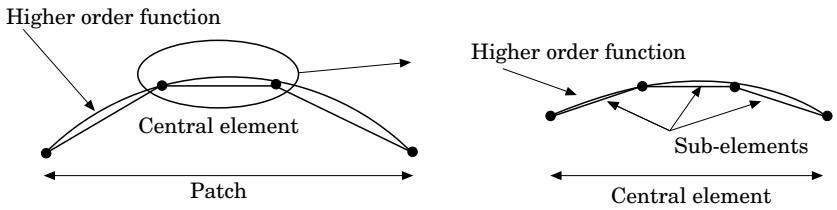

Figure 6. Definition of sub elements from patch interpolated function.

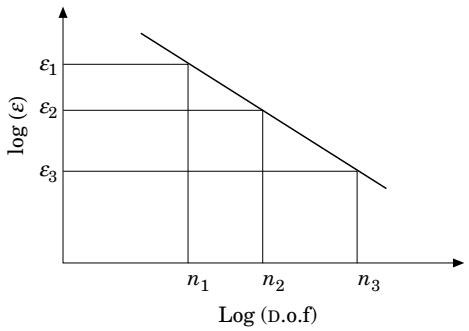

Figure 7. Uniform convergence of finite strip error.

As a plot forms a straight line, the gradient between two pairs of points can be calculated and equated.

$$\text{grad} = (\log(\varepsilon_2) - \log(\varepsilon_3))/(\log(n_2) - \log(n_3))$$
$$= (\log(\varepsilon_1) - \log(\varepsilon_3))/(\log(n_1) - \log(n_3)), \tag{15}$$
$$\log(\varepsilon_2/\varepsilon_3)/\log(n_2/n_3) = \log(\varepsilon_1/\varepsilon_3)/\log(n_1/n_3), \tag{16}$$
$$(\lambda_2 - \lambda_{EX})/(\lambda_3 - \lambda_{EX}))^{\beta} = (\lambda_1 - \lambda_{EX})/(\lambda_3 - \lambda_{EX}))^{\gamma}, \tag{17}$$

where $\beta = \log(n_1/n_3)$ and $\gamma = \log(n_2/n_3)$. The exact eigenvalue λ_{EX} can be solved simply using numerical techniques with a starting value equal to the eigenvalue having the highest number of degrees-of-freedom.

5. EXAMPLES

5.1. EXAMPLE 1: VIBRATION OF A SIMPLY SUPPORTED PLATE

A steel plate of width 100 mm and thickness 1·0 mm was examined for its natural frequency for a number of lengths of section varying from 10 mm to 1000 mm. The plate was simply supported along the sides. The minimum natural frequency occurs when the half wave length of the structure is the largest. Figure 8 is a plot of the natural frequency versus the half wave length of the structure. The natural frequency has been multiplied

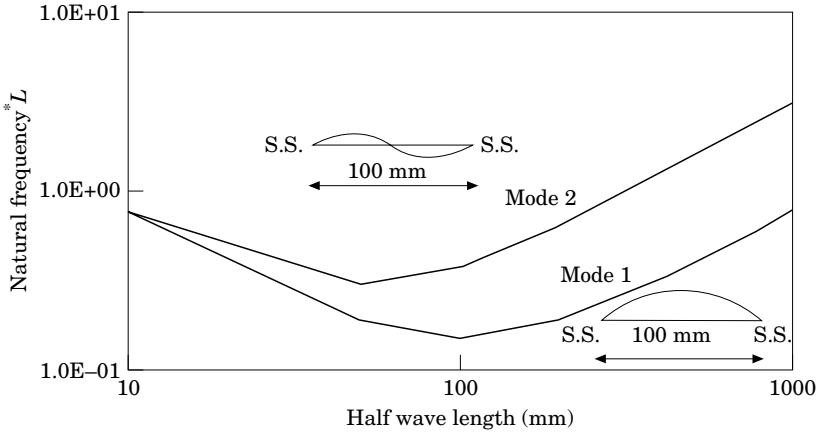

Figure 8. Finite strip results for the simply supported flat plate.

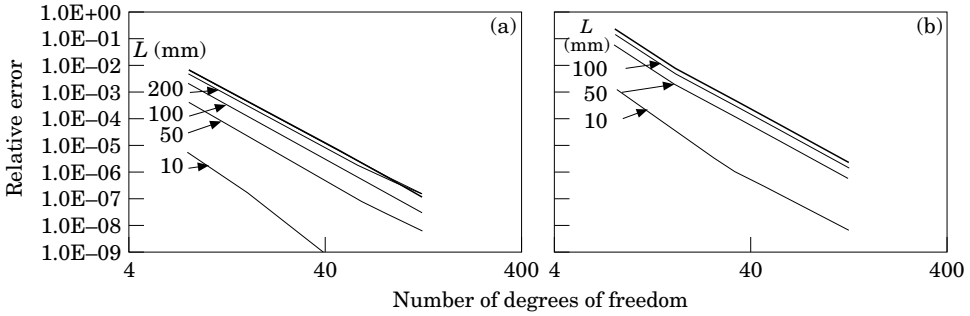

Figure 9. Finite strip errors for the simply supported flat plate of various lengths for modes 1 and 2. (a) mode 1; (b) mode 2.

by the length of the half wave length to produce a minimum point on the graph associated with the natural frequency for a square plate. That is, at a length of 100 mm for mode 1 and 50 mm for the double bubble in mode 2. Also on the figure is a sketch of the displacements of the plate

The plate was examined for a number of mesh refinements and an exact solution was derived. The errors for each mesh for both modes are plotted in Figure 9. The x-axis represents the number of degrees of freedom in the models used and the individual lines represent the error in the finite strip analysis for the various lengths of plate examined. The improved eigenvalues were calculated using the patch method described in this paper and using these values an error measure was determined for the finite strip analysis. The finite strip error, improved eigenvalue error and error measure have been plotted in Figure 10 for a couple of lengths and for the first two modes. The error for mode 2 is generally larger than that for mode 1. However, in all cases the improved eigenvalue is at least an order of magnitude more accurate than the finite strip results. As the improved

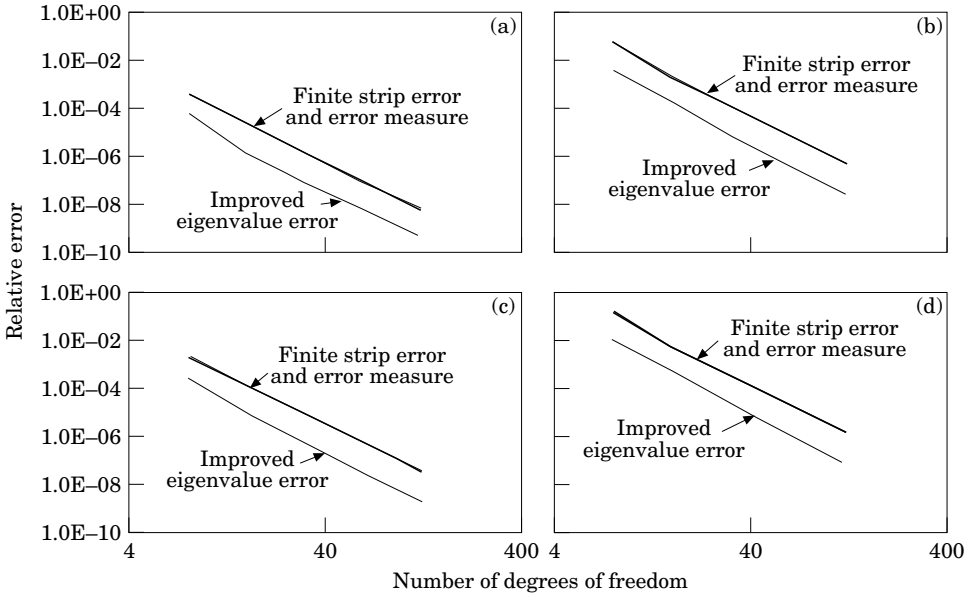

Figure 10. Finite strip errors, improved eigenvalue errors and error measures: (a) mode 1, $L = 50$ mm; (b) mode 2, L = 50 mm; (c) mode 1, $L = 100$ mm; (d) mode 2, L = 100 mm.

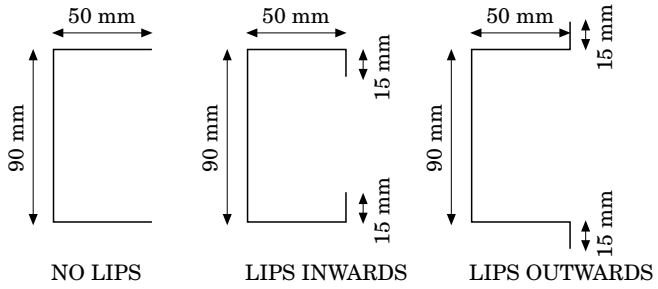

Figure 11. Dimensions of the three types of channels.

eigenvalue is quite accurate, the error measure for the finite strip solution using this value predicts accurately the error of the finite strip analysis.

5.2. EXAMPLE 2: VIBRATION OF CHANNEL SECTIONS

Three channel sections, of the same dimensions as used in reference [3] were examined using the finite strip method. The dimensions for the channels are given in Figure 11 with the thickness of the plate being 1·6 mm. These dimensions were also used by Lau and Hancock [10] for buckling analysis as they produce complex buckling modes that change from local buckling to distortional buckling to flexural and flexural-torsional buckling. The modes for the vibration of these sections follow a very similar path to that for the buckling.

The exact eigenvalues have been extrapolated from a number of refined meshes and have been plotted on the following figure for the first two modes for each of the three channels. The natural frequencies vary considerably with the length section changes as shown in Figure 12. This indicates that the section undergoes a variety of vibration modes as the length changes. These displaced modes are plotted in Figure 13. The shapes are identified on Figure 12.

Two meshes were examined for the prediction of the finite strip error. For each of these meshes the first two eigenvalues were examined and the results are shown in Figure 14. The improved eigenvalue was derived when the original central element was divided into 5 sub-elements. Previous work in reference [3] also used a sub-division of five elements.

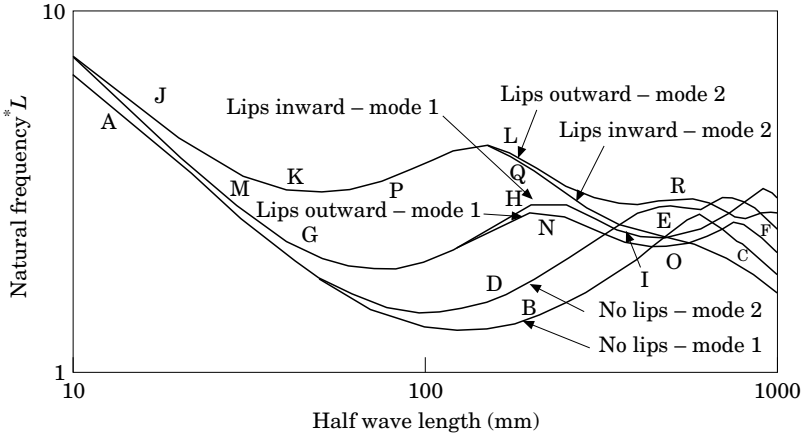

Figure 12. Finite strip results for the three channel sections. Letters indicate distorted shape in the following figure.

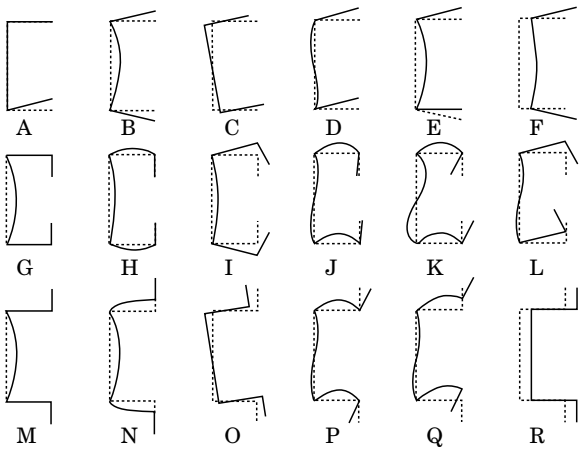

Figure 13. Distorted shapes of the vibrating channels. See previous figure for locations.

The additional time for the computation of the improved eigenvalue using 5 sub-elements is insignificant and the net result is much better.

The error graphs for the channel with the outward facing lips have not been shown in Figure 15 as they are virtually of an identical form as the error plots for the channel with the inward facing lips. The displacements for the vibrating channels in this paper are very similar to those for the buckling of these channels [3]. Hence, the finite strip errors, the improved eigenvalue errors and the error measures are virtually identical.

The large jump in each of the figures above around the half wave length of 700 mm, for the channel without the lips, and around 900 mm for the other channel occurs when the two modes have the same eigenvalue. From this point the modes swap over for the

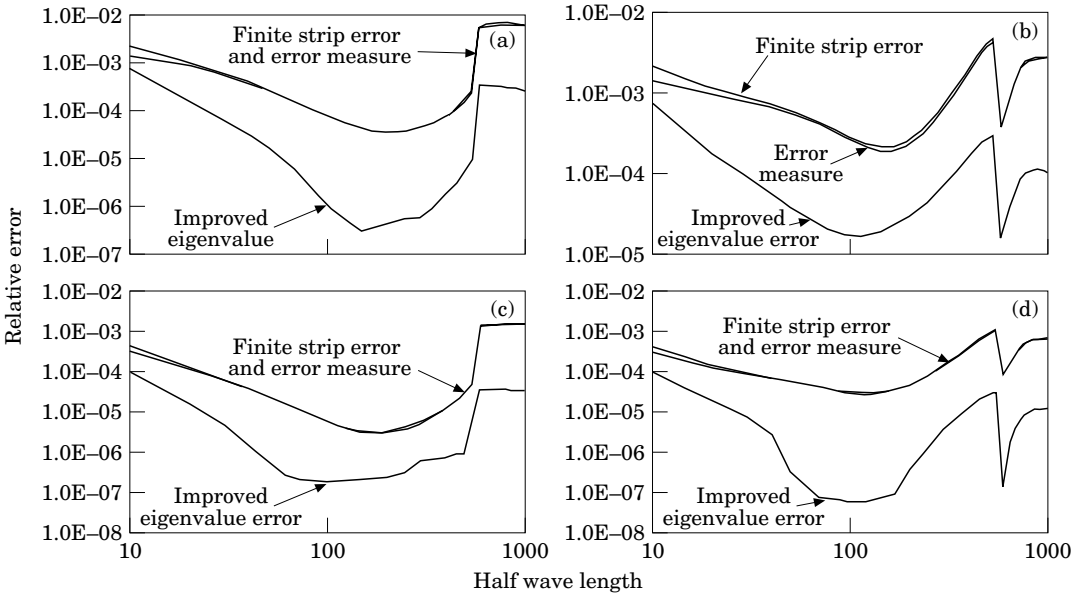

Figure 14. Finite strip errors, improved eigenvalue errors and error measures for the first two modes and different meshes. Channel with no lips: (a) mode 1, 68 d.o.f.; (b) mode 2, 68 d.o.f.; (c) mode 1, 132 d.o.f.; (d) mode 2, 132 d.o.f.

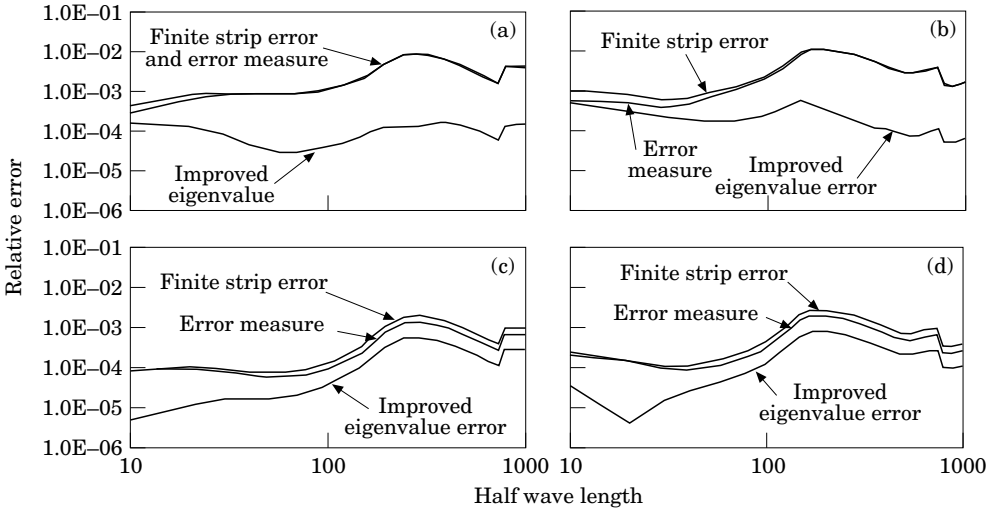

Figure 15. Finite strip errors, improved eigenvalue errors and error measures for the first two modes and different meshes. Channel with inward lips: (a) mode 1, 68 d.o.f.; (b) mode 2, 68 d.o.f.; (c) mode 1, 132 d.o.f.; (d) mode 2, 132 d.o.f..

lowest eigenvalue, and the natural frequency for the section. Even with such a sharp change in the figure, the error measure accurately predicts the finite strip error as it does so for all values of length.

6. CONCLUSION

The patch recovery method for the improved eigenvalue of a finite strip natural frequency analysis has been demonstrated in this paper to be highly accurate in predicting the error in the eigenvalue from finite strip analysis, with the improved eigenvalue being around two orders of magnitude more accurate than the original finite strip solution for the examples investigated in this paper. The method does not require the resolving of a finite strip model with a more refined mesh, and can be performed at an element level not requiring large global matrices to be formed. Hence this method is quite fast producing accurate results with little computation effort.

ACKNOWLEDGMENTS

The first author is supported financially by the Australian Postgraduate Research Award (Industry) in conjunction with G + D Computing of Sydney.

REFERENCES

1. Y. K. Cheung 1976 *Finite Strip Method in Structural Analysis*. New York: Pergamon Press Inc.
2. G. J. Hancock 1978 *Proceedings of ASCE* ST11 **104**, 1787–1799. Local, distortional, and lateral buckling of I-beams.
3. D. B. Stephen and G. P. Steven 1995 *ASCE Journal of Structural Engineering and Mechanics*. Error measures for the finite strip method.
4. P. O. Friberg 1986 *International Journal for Numerical Methods in Engineering* **23**, 91–98. An error indicator for the generalised eigenvalue problem using the hierarchical finite element method.

5. P. O. Friberg, P. Moller, D. Makovicka and N. E. Wiberg 1987 *International Journal for Numerical Methods in Engineering* **24**, 319–335. An adaptive procedure for eigenvalue problems using the hierarchical finite element method.
6. R. D. Cook 1991 *AIAA Journal* **29**, 1527–1529. Error estimation for eigenvalues computed from discretised models of vibrating structures.
7. J. Avrashi and R. D. Cook 1993 *Engineering Computations* **10**, 243–256. New error estimation for C^0 eigenproblems in finite element analysis.
8. D. B. Stephen and G. P. Steven 1996 *Computers and Structures* **61**, 747–761. Error estimation for plate buckling elements.
9. D. B. Stephen and G. P. Steven 1997 *Engineering Computations*, to be published. Error estimation for natural frequency analysis using plate elements.
10. S. C. W. Lau and G. J. Hancock 1987 *Proceedings of ASCE* **113**, 1063–1087. Distortional buckling formulas for channel columns.